THE JOURNAL OF BIOLOGICAL CHEMISTRY Vol. 280, No. 3, Issue of January 21, pp. 2378–2387, 2005
Printed in U.S.A.

Glycan-independent Role of Calnexin in the Intracellular Retention of Charcot-Marie-Tooth 1A Gas3/PMP22 Mutants*

Received for publication, May 7, 2004, and in revised form, November 2, 2004
Published, JBC Papers in Press, November 10, 2004, DOI 10.1074/jbc.M405104200

Alessandra Fontanini‡§, Romina Chies‡§, Erik L. Snapp¶, Moreno Ferrarini‖, Gian Maria Fabrizi‖, and Claudio Brancolini‡§**

From the ‡Dipartimento di Scienze e Tecnologie Biomediche, Sezione di Biologia and §MATI Center of Excellence, Universitá di Udine, Piazza le Kolbe 4, 33100 Udine, Italy, ¶Cell Biology and Metabolism Branch, NICHD, National Institutes of Health, Bethesda, Maryland 20892, and ‖Department of Neurological and Visual Science, Section of Clinical Neurology, Policlinico GB Rossi, Piazza le LA Scuro 1, 37134 Verona, Italy

Missense point mutations in Gas3/PMP22 are responsible for the peripheral neuropathies Charcot-Marie-Tooth 1A and Dejerine Sottas syndrome. These mutations induce protein misfolding with the consequent accumulation of the proteins in the endoplasmic reticulum and the formation of aggresomes. During folding, Gas3/PMP22 associates with the lectin chaperone calnexin. Here, we show that calnexin interacts with the misfolded transmembrane domains of Gas3/PMP22, fused to green fluorescent protein, in a glycan-independent manner. In addition, photobleaching experiments in living cells revealed that Gas3/PMP22-green fluorescent protein mutants are mobile but diffuse at almost half the diffusion coefficient of wild type protein. Our results support emerging models for a glycan-independent chaperone role for calnexin and for the mechanism of retention of misfolded membrane proteins in the endoplasmic reticulum.

Gas3/PMP22 encodes a tetraspan protein component of the compact myelin that is highly expressed in Schwann cells (1–3). Different genetic alterations in Gas3/PMP22 are responsible for a group of inherited neuropathies of the peripheral nervous system characterized by myelin dysfunction (4–6). Duplication of the Gas3/PMP22 gene is responsible for the majority of the Charcot-Marie-Tooth 1A (CMT1A)[1] disease, whereas loss of one allele of Gas3/PMP22 results in hereditary neuropathy with liability to pressure palsies, a mild variant of peripheral neuropathy (4, 5).

Point mutations in Gas3/PMP22 are also responsible for peripheral neuropathies (6, 7). Point mutations causing hereditary neuropathy with liability to pressure palsies result in either a premature termination of the translation or the synthesis of a longer altered protein (inherited peripheral mutation database IPNMDB, molgen-www.uia.ac.be/CMTMutations/). Other mutations are predicted to alter the splicing process and generate a nonfunctional protein. Overall, Gas3/PMP22 point mutations responsible for hereditary neuropathy with liability to pressure palsies cause a loss of function (8). Missense mutations localized in the transmembrane domains of the protein have been found in patients with the more severe forms of CMT1A and the Dejerine Sottas syndrome (6). Dejerine Sottas syndrome is characterized by an earlier age of onset and a more severe phenotype than CMT1A (9). The disease mechanism of the missense mutations is well established. These mutants are dominant gain of function mutations that impair the normal intracellular trafficking of the protein, causing intracellular accumulation of the protein in the endoplasmic reticulum (ER) or in the intermediate compartment. Moreover, Gas3/PMP22 mutants tend to form cytosolic aggresomes that may be protective (10–16). However, whether these misfolding mutations result in disease because of the oligomerization-dependent intracellular sequestration of the wild type (wt) form or by affecting the integrity and function of the ER is still debated (12, 17, 18).

Secreted and plasma membrane proteins are assembled into their native tertiary and quaternary structure in the ER. Incorrect assembly targets proteins for degradation (19–22). The lectins calnexin (CNX) and calreticulin (CRT) are critical elements of ER quality control for glycoproteins. These lectins interact with glycoproteins in the presence of monoglucosylated *N*-glycans (21). During maturation, glucosidase II removes the remaining glucose from the glycan, and interaction with lectin is terminated (20, 22–25). If the glycoprotein is correctly folded, it can exit the ER. If not, re-addition of a glucose to the *N*-linked glycan occurs by the action of a folding sensor: the UDP-glucose glycoprotein glucosyltransferase. Next, the glycoprotein is again recognized by CNX and CRT (20–22, 24). The CNX/CRT cycle prevents premature oligomeric assembly and export of misfolded glycoproteins from the ER (21).

Recently, it has demonstrated that Gas3/PMP22 interacts with CNX in sciatic nerves and that this interaction is prolonged in the case of mutant Gas3/PMP22 (18). This result suggested that sequestration by CNX may be relevant for CMT1A-related neuropathies. In this study, we have demonstrated that Gas3/PMP22 interacts with CNX in a glycan-dependent manner, whereas the CMT1A mutant Gas3/PMP22-L16P interacts with CNX in a glycan-independent manner. The glycan-independent interaction of CNX with Gas3/PMP22 occurs via the first transmembrane domain of the tetraspan. In addition, we also demonstrate that the L16P mutant fails to associate with membrane rafts and instead forms high molec-

* This work was supported by Ministero dell'Istruzione, dell'Università e della Ricerca Progetto COFIN-2002 (to C. B.). The costs of publication of this article were defrayed in part by the payment of page charges. This article must therefore be hereby marked "*advertisement*" in accordance with 18 U.S.C. Section 1734 solely to indicate this fact.

** To whom correspondence should be addressed. E-mail: cbrancolini@makek.dstb.uniud.it.

[1] The abbreviations used are: CMT1A, Charcot-Marie-Tooth 1A; ER, endoplasmic reticulum; GFP, green fluorescent protein; wt, wild type; CNX, calnexin; CRT, calreticulin; TX-100, Triton X-100; TM, transmembrane; CHAPS, 3-[(3-cholamidopropyl)dimethylammonio]-1-propanesulfonic acid; TRITC, tetramethylrhodamine isothiocyanate; FRAP, fluorescence recovery after photobleaching; ROI, region of interest; IP, immunoprecipitation; DTT, dithiothreitol; CFTR, cystic fibrosis transmembrane conductance regulator; VSVG, vesicular stomatitis virus glycoprotein.

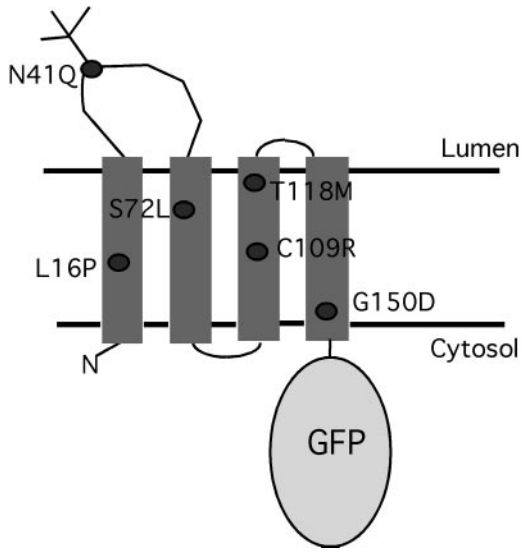

FIG. 1. **Schematic representation of the different Gas3/PMP22-GFP chimeras utilized.** The topology of Gas3/PMP22, as predicted by computer analysis, and the point mutations used are indicated. The *N*-glycosylation site is present at Asn^{41}. It is important to note that a non-tetraspan topology has been proposed by Taylor *et al.* (59).

ular weight oligomers by intermolecular disulfide bonds. Our results provide new insight into the mechanisms responsible for the intracellular retention of Gas3/PMP22 missense mutants.

EXPERIMENTAL PROCEDURES

Cell Culture—U2OS osteosarcoma cells, 293, and IMR90-E1A cells were grown in Dulbecco's modified Eagle's medium supplemented with 10% fetal calf serum, penicillin, and streptomycin. Transfection of cells was performed using the calcium phosphate precipitation method. U2OS cells stably expressing Gas3/PMP22, Gas3/PMP22-L16P, Gas3/PMP22-N41Q, and Gas3/PMP22-L16P/N41Q were selected for resistance to G418.

Microinjection and Time Lapse—Nuclear microinjection was performed using the Automated Injection System (Zeiss-Germany) as described previously (26). Different expression vectors were injected into the nuclei of cells for 0.5 s at a constant pressure of 50 hectopascals. For time-lapse analysis, cells were plated directly onto Petri dishes and observed shortly after microinjection. Time-lapse analysis was performed with a Leica TCS SP laser scanning microscope in a 5% CO_2 atmosphere at 37 °C.

Plasmid Construction—Fig. 1 schematically depicts the computer-predicted topology of Gas3/PMP22 and the different point mutants used in this study. For expression in eukaryotic cells, human *gas3/PMP22* and its point-mutated derivatives (13) were amplified by PCR and subcloned into pEGFP-N1 vector (Clontech). A sense primer (5′-GAGTGAATTCAACTCCGCTGAGCAGAACTT-3′) containing an EcoRI site and a reverse primer (5′-CGAGGATCCTCGCGTTTCCGCAAGATCA-3′) containing a BamHI site were used. The first transmembrane (TM) domains (TM1) of Gas3/PMP22 and Gas3/PMP22-L16P including four juxtamembrane amino acids (amino acids 1–34) were amplified by PCR and subcloned into pEGFP-N1 vector by using TM1up primer (5′-GAGTGAATTCAACTCCGCTGAGCAGAACTT-3′) containing an EcoRI primer and TM1down primer (5′-CATGTCGACGCGTGTCCATTGCCCAC-3′) containing a SalI site. All constructs generated were sequenced using an automated system (ABI PRISM 310) to check the fidelity of the inserted PCR fragments. The construction of mGFP-PSec61γ has been described previously (27).

Detergent Solubilization—Cells expressing wt or L16P were lysed on ice with 1% Triton X-100 (TX-100), 25 mM Hepes, pH 7.4, 150 mM NaCl, 1 mM phenylmethylsulfonyl fluoride, and 10 μg/ml each of aprotinin, leupeptin, antipain, and pepstatin at 4 °C for 30 min. The lysates were scraped from the dishes with a rubber policeman and centrifuged at 3,000 rpm for 10 min into a pellet and supernatant. To remove cholesterol before TX-100 extraction, cells were pretreated with 10 mM methyl-β-cyclodextrin in serum-free Dulbecco's modified Eagle's medium at 37 °C for 60 min.

Sucrose Gradient Fractionation—Sucrose gradient fractionation was performed as described previously (28). Monolayers of cells were lysed for 20 min in TNE/TX-100 buffer (20 mM Tris-HCl, pH 8.0, 150 mM NaCl, 5 mM EDTA, and 1% TX-100). Lysates were scraped from the dish and brought to 40% sucrose using 80% sucrose in TNE (20 mM Tris-HCl, pH 8.0, 150 mM NaCl, and 5 mM EDTA) without TX-100. A linear sucrose gradient (5–30% in TNE without TX-100) was layered over the lysates in an ultracentrifuge tube. Gradients were centrifuged for 18 h at 40,000 rpm at 4 °C in a TST 35.5 Beckman rotor. Fractions were precipitated in 80% acetone, and pellets were solubilized in SDS buffer. The pellet from the bottom of the tube was solubilized by SDS buffer and loaded as insoluble pellet.

Immunoprecipitation—Cells were extracted in lysis buffer (150 mM NaCl, 50 mM Tris-HCl, pH 7.5, and 1% CHAPS containing 1 mM phenylmethylsulfonyl fluoride and 10 μg/ml each of aprotinin, leupeptin, antipain, and pepstatin), and after centrifugation at 10,000 rpm for 10 min, the anti-GFP antibody (29) was added. After 3 h on ice, protein A-Sepharose (Amersham Biosciences) was added, and incubation was prolonged for 1 h on ice. After a brief centrifugation in an Eppendorf centrifuge, immunoprecipitates were washed four times with lysis buffer. Immunocomplexes were released by boiling for 5 min in SDS sample buffer and separated by SDS-PAGE on a 10% gel.

Immunofluorescence and Photobleaching Experiments—For immunofluorescence microscopy, cells were fixed with 3% paraformaldehyde in phosphate-buffered saline for 20 min at room temperature and permeabilized with 0.1% TX-100. Coverslips were labeled with either anti-calnexin (Transduction Laboratories) or anti-calreticulin (StressGen) followed by TRITC-conjugated anti-mouse and anti-rabbit secondary antibodies (Sigma). Cells were imaged with a Leica TCS SP microscope with a 488–534 λ Ar laser and a 633 λ HeNe laser. Fluorescence recovery after photobleaching (FRAP) experiments were performed on a temperature- and CO_2-controlled stage with a Leica TCS SP confocal microscope using the 488 nm and 518 nm lines of the Ar laser with a 63 × 1.4 NA oil objective. FRAP experiments were performed by photobleaching a 12.5 × 12.5-μm region of interest (ROI) at full laser power. D_{eff} was determined using an inhomogeneous diffusion simulation (30). The mobile fraction (M_f) was calculated as described previously (31). Image analysis was performed using Metamorph 6.04 (Universal Imaging Corp.).

Immunoblotting and Enzymatic Treatments—Proteins were transferred to nitrocellulose membranes (pore size, 0.2 μm; Schleicher and Schuell) using a semidry blotting apparatus (Amersham Biosciences). Membranes were incubated overnight at room temperature with anti-GFP, anti-calnexin (Transduction Laboratories), anti-ERp44 (32), anti-ERp57 (Stressgen), anti-N-cadherin (Sigma), anti-PDI (Transduction Laboratories), or anti-p62 (Transduction Laboratories) primary antibodies followed by peroxidase-conjugated anti-rabbit (Sigma) or goat anti-mouse (Euroclone) secondary antibodies. Blots were developed with Super Signal West Pico or Dura, as recommended by the vendor (Pierce).

PNGaseF treatment of cellular lysates and immunoblotting analyses were performed as described previously (33). For endoglycosidase H treatment, the cellular lysates were prepared in 0.5% SDS and 1% β-mercaptoethanol and denatured by boiling for 10 min, and then 50 mM sodium acetate, pH 5.5, and 1% Nonidet P-40 were added. After the addition of 1 milliunit of endoglycosidase H (EndoH; Roche Applied Science), samples were incubated for 3 h at 37 °C.

RESULTS

CNX Interacts with Gas3/PMP22 and Gas3/PMP22-L16P—CNX is a non-glycosylated type I membrane resident ER protein, and it represents a major component of the molecular chaperone system, which ensures exit from the ER of correctly folded proteins (34). CNX contains a lectin site with specificity for the oligosaccharide-processing intermediate $Glc_1Man_9GlcNAc_2$. Unlike classical chaperones, CNX is proposed to retain the unfolded glycoproteins and to coordinate the activities of other ER chaperones such as ERp57.

Recent studies have demonstrated that CNX can interact with both wt and misfolded Gas3/PMP22 in sciatic nerves (18). To investigate the ability of CNX to interact with Gas3/PMP22 and the point mutant L16P responsible for CMT1A, we employed co-immunoprecipitation (IP) experiments. Cells stably expressing wt or L16P were lysed, and the same amounts of proteins were immunoprecipitated using an anti-GFP antibody. Immunoblots of the IP eluates were probed with an

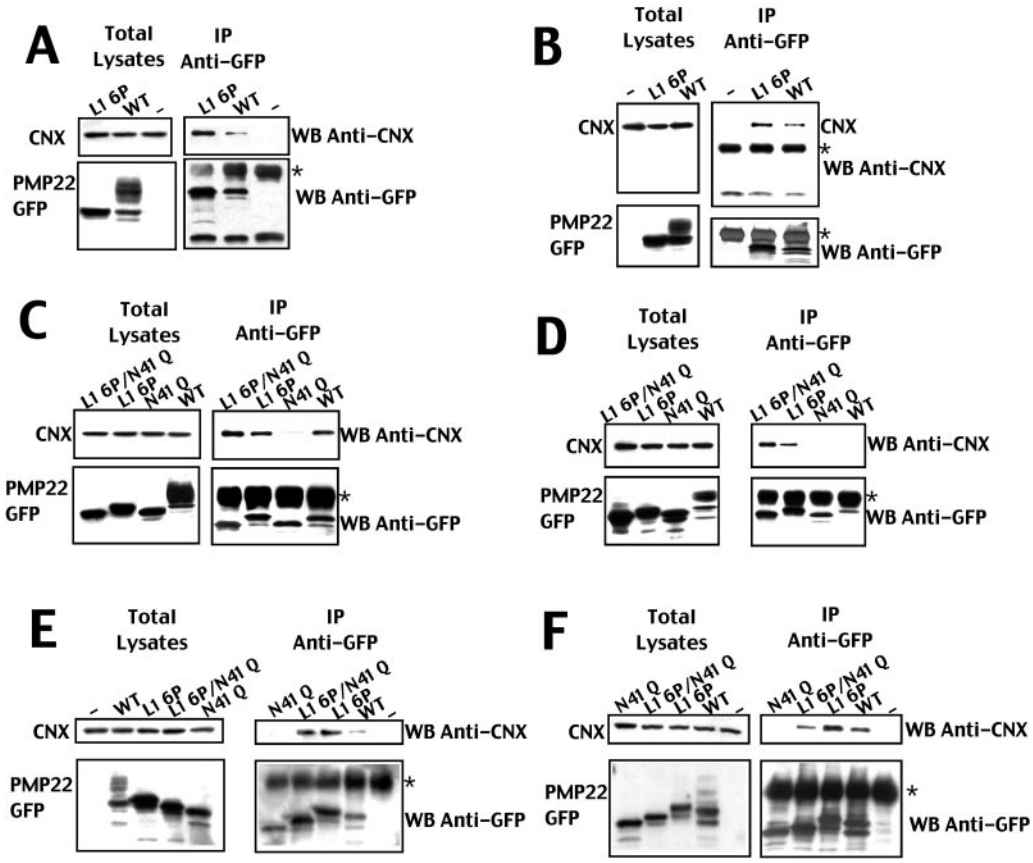

FIG. 2. **CNX interacts with Gas3/PMP22.** *A* and *B*, lysates produced from cells stably (*A*) or transiently (*B*) transfected with wt, L16P, or an empty vector (−). Immunoblots of total lysates were performed against CNX (as loading control) and GFP (for transfection efficiency). IPs were performed from the same lysates using anti-GFP antiserum. The immunocomplexes were resolved by SDS-PAGE and immunoblotted with anti-CNX or anti-GFP as indicated. Throughout this figure, the *asterisk* indicates IgG cross-reactivity. *C* and *D*, lysates were produced from transiently (*C*) or stably (*D*) transfected cells expressing wt, N41Q, L16P/N41Q, and L16P. Immunoblots of total lysates were performed against CNX (as loading control) and GFP (*C* and *D*) for transfection efficiency. IPs were performed using anti-GFP antiserum. The immunocomplexes were resolved by SDS-PAGE and immunoblotted with anti-CNX or anti-GFP as indicated. *E* and *F*, lysates produced from IMR90-E1A cells (*E*) or 293 cells (*F*) transiently transfected with wt, L16P, N41Q, or L16P/N41Q. Immunoblots of total lysates were performed against CNX (as loading control) and GFP (for transfection efficiency). IPs were performed from the same lysates using anti-GFP antiserum. The immunocomplexes were resolved by SDS-PAGE and immunoblotted with anti-CNX or anti-GFP as indicated.

anti-CNX antibody. Fig. 2*A* reveals that, at steady state, the misfolded mutant L16P strongly interacts with CNX, whereas Gas3/PMP22 only weakly interacts with this lectin. As expected, in total lysates loaded to verify transfection efficiency, the wt was present as a doublet representing the pre-Golgi and post-Golgi forms, whereas L16P was detected solely as the pre-Golgi form (see Fig. 4*A* for a detailed characterization). Immunofluorescence studies confirmed that in stably transfected cells, the vast majority of wt was exposed on the cell surface, whereas the L16P mutant was retained in the ER (data not shown).

Because the majority of wt Gas3/PMP22 in stably transfected cells trafficked to the cell surface, we investigated whether newly synthesized wt protein was able to interact with CNX, similarly to the misfolded mutants when present in the ER. To this end, we performed anti-CNX co-IPs of lysates of transiently transfected cells expressing wt or L16P constructs, 30 h after transfection. Under these conditions, consistent amounts of wt could be detected as a pre-Golgi form (Fig. 2*B*), similar to the L16P mutant.

The same amounts of cellular lysates were immunoprecipitated using an antibody against GFP. After electrophoretic separation, the immunoblots were probed with anti-CNX antibody. Fig. 2*B* demonstrates that both wt and L16P interact with CNX. The same blot was also probed with an antibody against GFP to demonstrate that wt and L16P were immunoprecipitated with similar efficiencies. In total lysates, wt was present as a doublet of bands representing the pre- and post-Golgi forms. These results suggest that wt only transiently associates with CNX, whereas the misfolded ER-retained mutant L16P forms a stable complex with CNX.

CNX Interacts with Gas3/PMP22 in a Glycan-dependent Manner and with Gas3/PMP22-L16P in a Glycan-independent Manner—Folding substrates interact with CNX via their monoglucosylated *N*-linked glycans (23, 35). However, some reports have indicated that CNX can bind to polypeptide segments of both glycosylated and non-glycosylated proteins (36–39). To investigate whether Gas3/PMP22-CNX interactions are glycan-independent or -dependent, we utilized the glycosylation-defective mutants N41Q and L16P/N41Q.

Cells transiently transfected with wt, the single mutants L16P and N41Q, or the double mutant L16P/N41Q were lysed and immunoprecipitated using an anti-GFP antibody. After electrophoretic separation, the immunoblots were probed with anti-CNX antibody. Surprisingly, Fig. 2*C* shows that only the glycosylation-defective mutant N41Q was unable to interact with CNX, whereas the double mutant L16P/N41Q efficiently formed a complex with CNX. The same blot was also analyzed with anti-GFP antibody to confirm that the pre-Golgi forms of wt and L16P, L16P/N41Q, and N41Q mutants were similarly immunoprecipitated.

We observed similar results in stably transfected cells. The

double mutant L16P/N41Q was recognized by anti-CNX, similar to L16P (Fig. 2*D*). In stably transfected cells, a reduced amount of pre-Golgi wt protein was detected by co-IP, and therefore, interaction with CNX was barely detectable. The interaction between L16P/N41Q and CNX was consistently observed in 10 different co-IP experiments and by using different detergents such as CHAPS and Triton X-100. Furthermore, binding to CNX was similarly observed when L16P/N41Q was fused to the shorter FLAG tag instead of the GFP, and IPs were performed with the anti-FLAG antibody (data not shown).

Next, we investigated whether the double mutant L16P/N41Q was able to interact with CNX in other cell lines. IMR90-E1A and 293 cells transiently transfected with wt, single mutants L16P and N41Q, or the double mutant L16P/N41Q were lysed and immunoprecipitated using the anti-GFP antibody. After electrophoretic separation, the immunoblots were probed with anti-CNX antibody. Fig. 2, *E* and *F*, reveals that the double mutant L16P/N41Q efficiently formed a complex with CNX in 293 and IMR90-E1A cells. Curiously, in 293 cells, it seems that the L16P/N41Q mutant was less efficient in binding CNX than the L16P mutant. The same blot was also analyzed with anti-GFP antibody to confirm that the pre-Golgi forms of wt and L16P, L16P/N41Q, and N41Q mutants were similarly immunoprecipitated.

N-Glycosylation Is Not Required for Intracellular Retention and Aggresome Formation by Misfolded Gas3/PMP22 Mutants—Gas3/PMP22-L16P exhibits trafficking defects (10, 12, 13) and accumulates in the ER (10, 18), where it can form aggresomes (18, 40, 41). Therefore, we asked whether *N*-glycosylation plays a role in the ER retention and aggresome formation of Gas3/PMP22 mutants. Immunofluorescence analysis for GFP and CNX was performed in U2OS cells transiently expressing wt, the single mutant L16P, or the double mutant L16/N41Q (Fig. 3). The wt protein was exported to the cell surface and triggered the formation of endocytotic vacuoles that did not co-localize with CNX, similar to previous results (26). Both of the mutated proteins were retained in the ER and formed aggresome structures. This result confirmed that *N*-glycosylation is not required for the formation of aggresomes by ER-retained proteins (42). Interestingly, not all of the aggresomes induced by L16P were positive for CNX (Fig. 3, *arrowheads*). This heterogeneous pattern of CNX localization within the aggresomes was more evident for the glycan-defective mutant L16/N41Q. The heterogeneity may reflect differences in aggresome maturity.

Similar results were obtained when immunofluorescence studies were performed in IMR90-E1A and 293 cells (data not shown).

Gas3/PMP22-L16P Fails to Associate with Membrane Rafts—At steady state, wt is present as three distinct bands on an immunoblot (Fig. 4*A*). Enzymatic treatments with PNGaseF and endoglycosidase H demonstrate that the faster migrating band is a deglycosylated form, whereas the intermediate band represents the pre-Golgi form, and the slow migrating band is the post-Golgi, mature form of Gas3/PMP22. Surprisingly, the co-IP studies in Fig. 2 suggest that wt, immunoprecipitated under native conditions, is present primarily as an immature form with the same electrophoretic profile as the pre-Golgi mutant L16P (see Fig. 2). Given that the wt protein reaches the cell surface, we considered the possibility that the post-Golgi form of wt was not immunoprecipitated under our experimental conditions.

Recent studies have indicated an association of Gas3/PMP22 with glycosphingolipid/cholesterol-enriched membranes, also known as lipid rafts (43, 44). We postulated that the failure to immunoprecipitate the mature form of wt under non-denaturing conditions could be dependent on its tight association with lipid rafts, which might render it insoluble under the experimental conditions used.

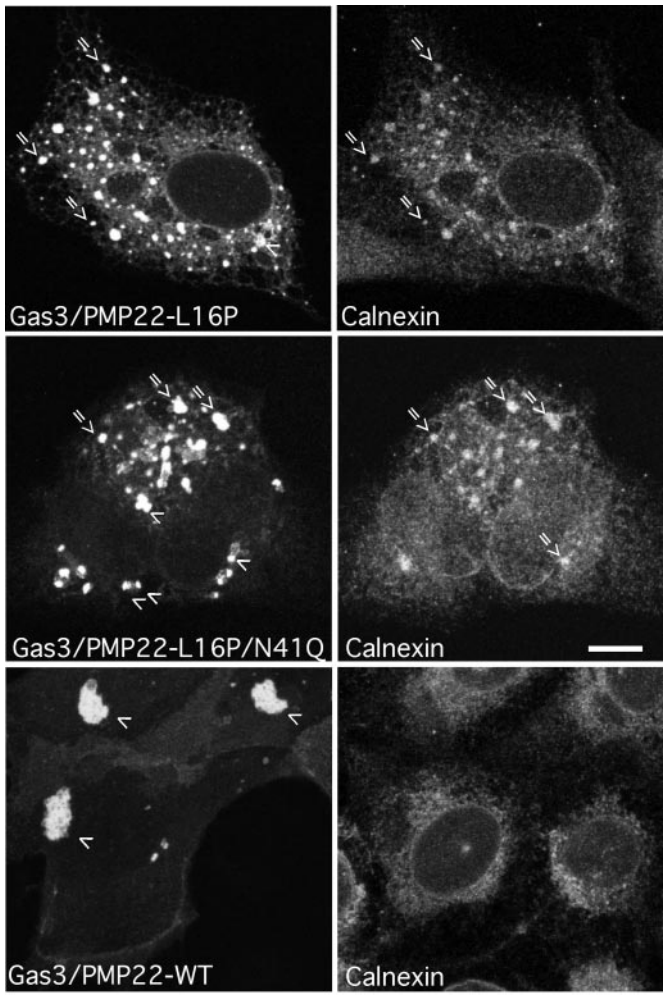

FIG. 3. **The role of *N*-glycan in the subcellular localization of the L16P mutant.** Immunofluorescence analysis of cells expressing wt Gas3/PMP22, Gas3/PMP22-L16P, and Gas3/PMP22-L16P/N41Q mutants fused to GFP. Transiently transfected cells were fixed and labeled with anti-calnexin. In Gas3/PMP22-L16P and Gas3/PMP22-L16P/N41Q, *arrows* point to aggresomes that co-localize with CNX, whereas *arrowheads* point to aggresomes that do not co-localize with CNX. For wt Gas3/PMP22, *arrowheads* point to endocytic vacuoles that do not co-localize with CNX. *Bar*, 10 μm.

First, we analyzed the detergent solubility of wt and the L16P mutant. Stably transfected cells were extracted for 30 min on ice with 1% TX-100 (see "Experimental Procedures"). Detergent-soluble and insoluble materials were separated by centrifugation. Consistent with the Triton insolubility of raft-associated proteins, wt fractionated with the Triton-insoluble membrane fraction, whereas L16P was largely soluble (Fig. 4*B*).

Cholesterol is an important structural component of lipid rafts and maintenance of the raft microenvironment is sensitive to cholesterol depletion (45). Methyl-β-cyclodextrin is commonly used to verify the association with lipid rafts of different proteins (43, 44). After cholesterol depletion (Fig. 4*B*, *MβCD*), Gas3/PMP22-wt was fractionated with the soluble fraction, similarly to L16P mutant. This result provided additional evidence for the association of mature wt with lipid rafts.

To confirm the association of Gas3/PMP22 with membrane rafts, we performed centrifugation to equilibrium on a sucrose density gradient (28). Triton lysates, adjusted to 40% sucrose,

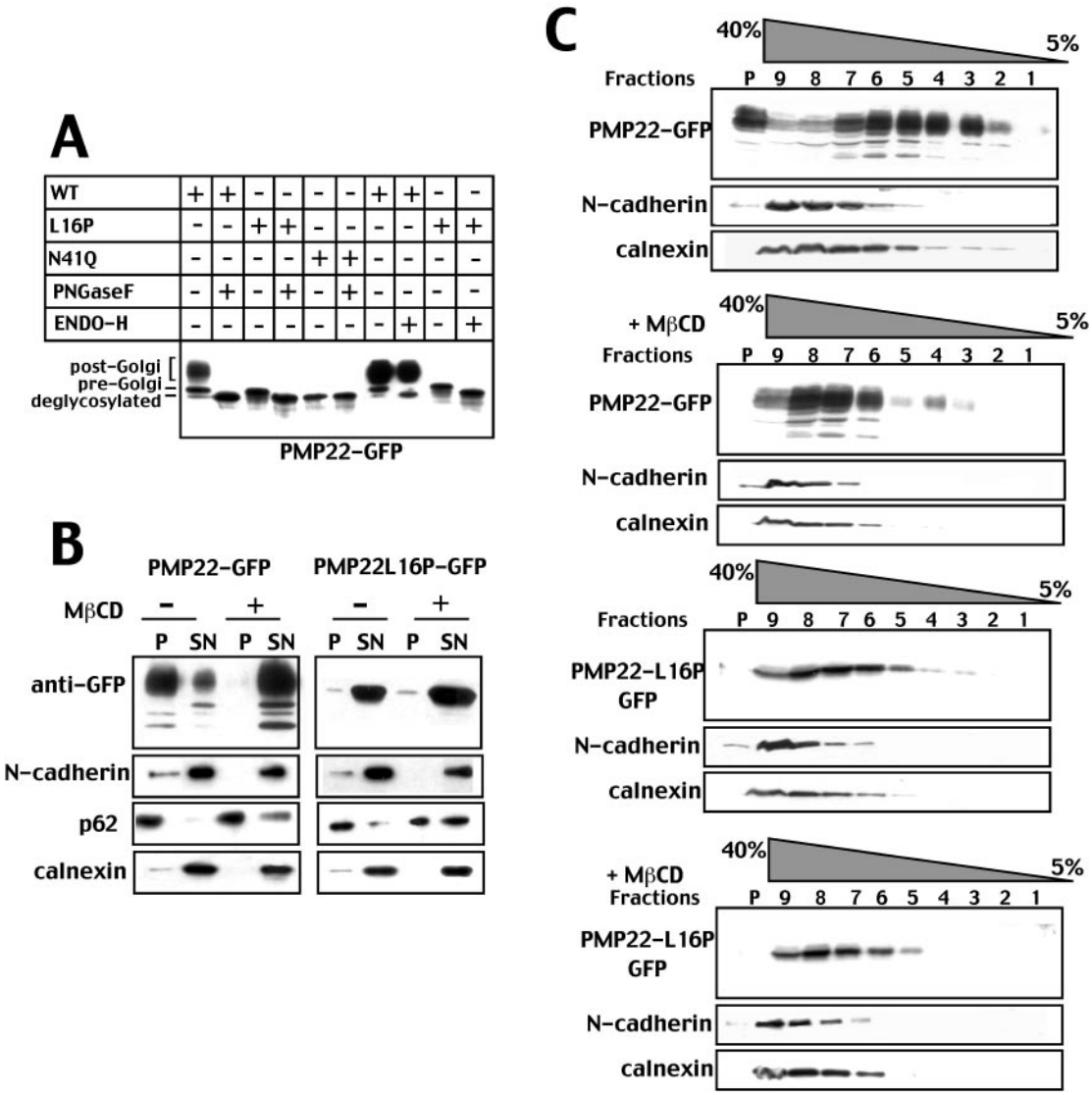

FIG. 4. **L16P fails to associate with lipid rafts.** *A*, characterization of the GFP-tagged wt, N41Q, and L16P in cells stably expressing them. Immunoblots were performed using an anti-GFP antibody. Cellular lysates were treated with PNGaseF or endoglycosidase H. *B*, cells stably expressing wt or L16P were lysed in TX-100 buffer to fractionate soluble (*SN*) and insoluble (*P*) proteins as described under "Experimental Procedures." Immunoblots were performed using the indicated antibodies. *C*, cells stably expressing wt or L16P were lysed in TNE/TX100 buffer. Lysates were adjusted to 40% sucrose, and sucrose gradients (5–30%) were formed over them (28). *P*, sucrose gradient pellet. Fraction 9 is from the bottom of the gradient. Cells were treated with methyl-β-cyclodextrin (*MβCD*) as indicated. Immunoblots were performed using the indicated antibodies.

were layered at the bottom of a 5–30% sucrose gradient. Fraction 9 was at the bottom of the gradient, and fraction 1 was at the top. Wt was found throughout the gradient but was primarily found in the low-density fractions 3–7 and in the pellet (*P*), probably in the form of aggregates. (Fig. 4*C*). Upon methyl-β-cyclodextrin treatment, wt was shifted to the bottom of the gradient (fractions 6–9), and the pellet fraction was dramatically reduced. This result suggests that the aggregation of wt depends on the presence of cholesterol and lipid rafts. N-cadherin and calnexin controls remained at the bottom of the gradient (fractions 6–9), as expected for solubilized proteins. In contrast, L16P was detected at the bottom of the gradient (fraction 5–9), but not in the pellet, irrespective of the presence of methyl-β-cyclodextrin (Fig. 4*C*). Thus, mature Gas3/PMP22, but not the CMT1A mutant, can associate with lipid rafts.

Disulfide Bonds Stabilize the Oligomeric Forms of the ER-retained Mutants—Aggregation of misfolded proteins in the ER can trigger the formation of interchain disulfide bonds (46, 47). We investigated whether misfolded Gas3/PMP22 oligomer formation involved interchain disulfide bonds. Cell lysates expressing wt, L16P, and L16P/N41Q were prepared under both non-reducing and reducing conditions and separated by SDS-PAGE on non-reducing or reducing gels. Under reducing conditions, L16P, L16P/N41Q, and wt migrated as bands of the expected size between M_r 42,000 and M_r 50,000. In non-reducing gels, additional high molecular weight bands (M_r 90,000 and M_r 130,000) were observed for L16P (Fig. 5*A*). In contrast, the wt form showed the same electrophoretic pattern as seen in reducing gels (Fig. 5*A*). L16P/N41Q resolved under non-reducing conditions also exhibited additional high molecular weight bands at M_r 90,000, M_r 130,000, and higher molecular weights, which migrated slightly faster than L16P, probably due to the absence of the sugar moiety (see Fig. 5*A*). Disulfide bond-dependent oligomer formation was not a consequence of the GFP because oligomers were also detected when L16P was tagged with the FLAG epitope (data not shown).

It is possible that the high molecular weight bands represent misfolded Gas3/PMP22 mutants linked to ER thioreductases.

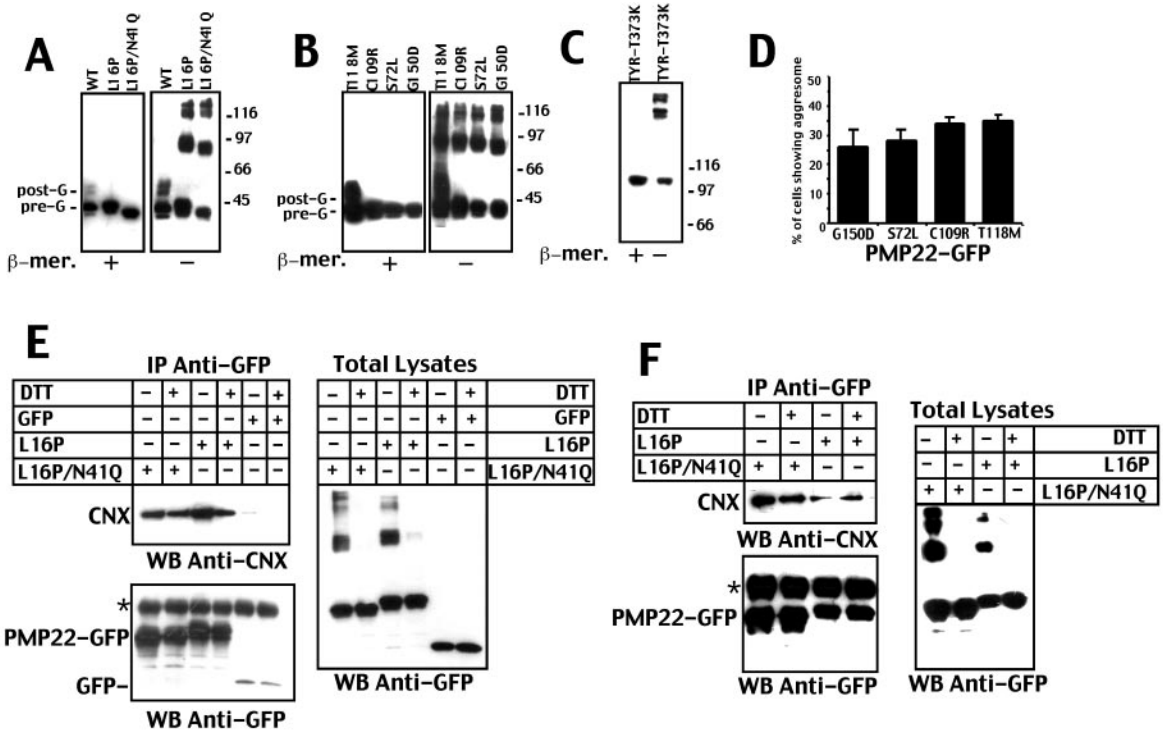

FIG. 5. **Disulfide bond formation and oligomerization of Gas3/PMP22 mutants.** *A* and *B*, cellular lysates from cells transiently expressing wt or the indicated point mutants were separated by SDS-PAGE under reducing or non-reducing conditions as indicated. The pre- and post-Golgi forms of wt are indicated by *pre-G* and *post-G*. *C*, cellular lysates from cells transiently expressing the TYR (T373K) point mutant were separated by SDS-PAGE electrophoresis under reducing or non-reducing conditions as indicated. *D*, cells transiently expressing the indicated point mutants were fixed and scored for the appearance of aggresomes by fluorescence microscopy. Data represent arithmetic means ± S.D. of three independent experiments. *E* and *F*, cellular lysates from cells transiently (*E*) or stably (*F*) transfected with the indicated Gas3/PMP22 cDNAs and grown in the absence or presence of DTT. Anti-GFP immunoblots of total lysates reveal high molecular weight oligomers. IPs were performed from the same lysates using anti-GFP antiserum. The immunocomplexes were immunoblotted with anti-CNX or anti-GFP as indicated. *, IgG cross-reactivity.

However, we were unable to detect PDI, ERp57, and ERp44 in higher molecular weight bands from lysates isolated from cells expressing misfolded Gas3/PMP22 mutants by immunoblots (data not shown).

Next, we asked whether the formation of interchain disulfide bonds is a common event for misfolded Gas3/PMP22 point mutants. Expression of the ER-retained mutants S72L, C109R, G150D, and T118M induces the formation of aggresomes (Fig. 5*D*). The S72L, C109R, and G150D mutants form interchain disulfide bonds, which generate high molecular weight oligomers (Fig. 5*B*). Interestingly, the T118M mutant displayed intermediate properties among the wt and the ER-retained mutants tested. T118M can be detected both as a mature post-Golgi form similar to the wt and as high molecular weight oligomers characteristic of ER-retained mutants (Fig. 5*B*). The presence of T118M both at the cell surface and in the ER as oligomers is consistent with previously reported abnormalities in the trafficking of this mutant when expressed *in vitro* (11). It remains unclear whether the T118M mutation represents a functionally irrelevant polymorphism or whether it can act as a pathogenic Charcot-Marie-Tooth mutation.

The formation of interchain disulfide bonds is not a specific response to the misfolding of Gas3/PMP22 in the ER. When the ER-retained mutant of the tyrosinase TYR (T373K) (48) was expressed in cells and cellular lysates were separated under non-reducing conditions, high molecular weight oligomers were observed for the TYR-T373K mutant (Fig. 5*C*). This suggested that the formation of interchain disulfide bonds may be a more general response for misfolded transmembrane proteins.

Given these results, we next asked whether the glycan-independent interaction of L16P with CNX requires the generation of high molecular weight oligomers. Cells were transiently transfected with L16P, L16P/N41Q, or GFP alone and treated with dithiothreitol (DTT) for 30 min before cell lysis. DTT treatment led to the disappearance of high molecular weight oligomers (Fig. 5*E*). However, the ability of L16P and L16P/N41Q to interact with CNX was unaffected by the reduction of disulfide bonds (Fig. 5*E*). The ability of CNX to interact with L16P and L16P/N41Q independently of high molecular weight oligomers also was confirmed in stably transfected cells (Fig. 5*F*). Therefore, ER-retained mutants of Gas3/PMP22 oligomerize by interchain disulfide bonds, but this oligomerization does not explain the glycan-independent interaction of these mutants with CNX.

Calnexin Binds to the First Transmembrane Domain of Gas3/PMP22—Recently, it has been demonstrated that CNX can stably bind to an isolated transmembrane domain of proteolipid protein in a glycan-independent manner (39). We investigated whether CNX interacts with misfolded L16P by a similar mechanism. We generated truncated versions of wt and L16P encoding a short cytoplasmic domain and the first transmembrane domain, TM1 (amino acids 1–34), fused to GFP. When expressed in cells, both wt TM1 and L16P TM1 accumulated in the ER (Fig. 6*A*) and induced the formation of aggresome-like fluorescent accumulations (Fig. 6*B*).

To directly assess the ability of these single transmembrane domains to interact with CNX, we performed co-IP experiments. Both wt and L16P TM1 associated with CNX (Fig. 6*C*). This result provides new molecular details of the glycan-independent interaction of CNX with misfolded L16P mutants. In addition, the results indicate that TM1, expressed alone, is recognized as misfolded and interacts in a glycan-independent manner with CNX. Thus, CNX appears to recognize an "unassembled" TM domain of a polytopic protein as misfolded (39).

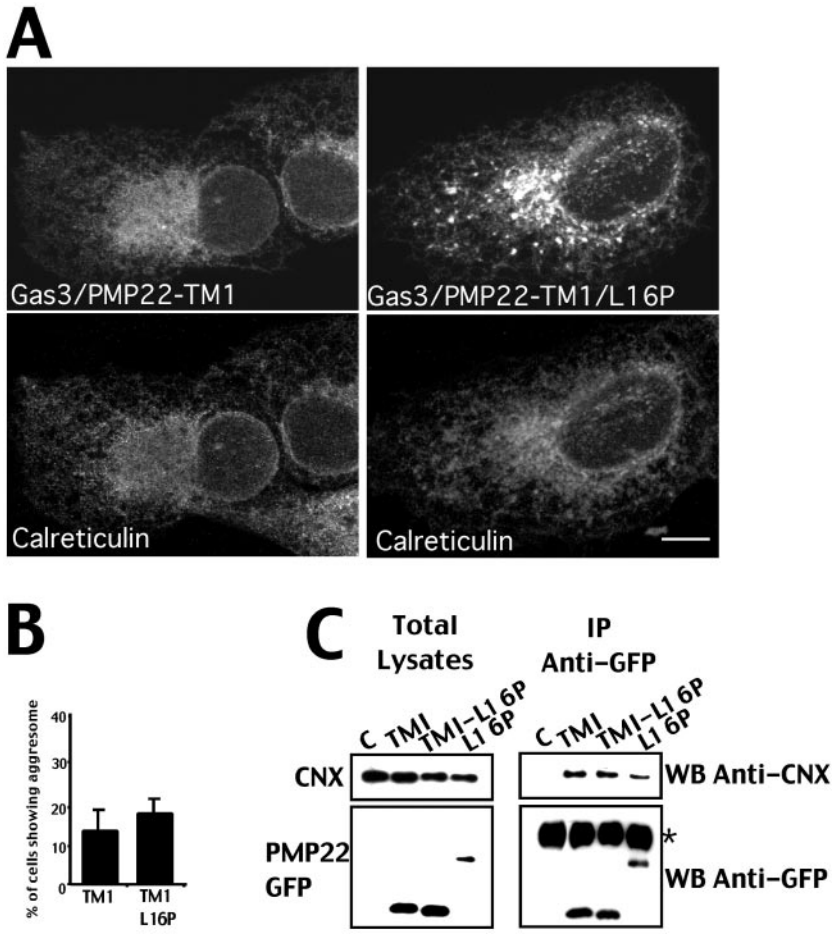

FIG. 6. **Calnexin binds to the first transmembrane domain of Gas3/PMP22.** *A*, immunofluorescence analysis of cells expressing the first transmembrane domain of wt (*TM1*) or of the L16P mutant (*TM1/L16P*) fused to GFP. Cells were fixed and labeled with anti-calreticulin antibody. *Bar*, 10 μm. *B*, cells transiently expressing the indicated Gas3/PMP22 transmembrane domains were fixed and scored for the appearance of aggresomes by fluorescence microscopy. Data represent arithmetic means ± S.D. of three independent experiments. *C*, cell lysates were harvested from cells transiently transfected with TM1, TM1-L16P, or L16P as a positive control or from untransfected cells as a negative control (*lane C*). Anti-CNX and anti-GFP immunoblots of total lysates were performed. IPs were performed from the same lysates using anti-GFP antiserum. The immunocomplexes were immunoblotted with anti-CNX or anti-GFP as indicated. *, IgG cross-reactivity.

Diffusional Mobility of Wt and Mutant Gas3/PMP22-GFP within ER Membranes—The failure of the different Gas3/PMP22 misfolded mutants to exit the ER, their assembly into high molecular weight oligomers, and their stable interaction with the quality control machinery prompted us to investigate the mechanism of ER retention. Is the mutant immobilized in the ER, or is it sequestered away from ER exit sites by the quality control machinery? To distinguish between these possibilities, we assessed the mobility of the different mutants in live cells using FRAP. The different cDNAs were microinjected into the nucleus, and the cells were subjected to FRAP analysis within 2 h, before the formation of aggresomes. To measure the mobility of wt in the ER, cells were treated with brefeldin A shortly after microinjection to retain wt in the ER. In all FRAP experiments, a strip ROI across the ER was photobleached with intense laser light, and images were collected with reduced laser intensity to monitor the movement of the different unbleached GFP fusion proteins into the ROI. Qualitative analysis of cells expressing wt or L16P revealed that FRAP recoveries were rapid and diffusive (Fig. 7).

Surprisingly, quantitative analysis of the recovery kinetics revealed a dramatic difference between the mobilities of wt and the misfolded mutants (Table I). Wt diffuses with an effective diffusion coefficient (D_{eff}) of 0.54 ± 0.14 $\mu m^2/s$, and 94 ± 7% of the molecules were mobile. These results were similar to those for the highly mobile resident ER membrane protein mGFPSec61γ (D_{eff} = 0.51 ± 0.15 $\mu m^2/s$) and the glycosylation-defective N41Q mutant (0.64 ± 0.08 $\mu m^2/s$), which is not recognized by CNX. The value for mGFPSec61γ is comparable with the previously reported value of 0.53 $\mu m^2/s$ (27).

In contrast, the D_{eff} values of the two misfolded mutants L16P and L16P/N41Q were significantly lower (0.29 ± 0.07 and 0.28 ± 0.12 $\mu m^2/s$, respectively). Additional misfolded mutants (G150D, S72L, and C109R) also exhibited significantly slower D_{eff} values relative to wt (Table II). No significant differences were observed for any of the M_f values (Tables I and II).

The dramatic reduction in mobility of the misfolded mutants is in contrast to the unaltered diffusion coefficients of other misfolded membrane proteins as observed by Nehls *et al.* (49) for misfolded VSVG and by Haggie *et al.* (50) for misfolded CFTR. However, PMP22 is similar to both VSVG and CFTR in that the misfolded proteins are retained in the ER, despite being mobile.

D is relatively insensitive to small changes in the radius of a molecule (30). Diffusion of a molecule in a membrane is proportional to the log of the radius of a molecule (51). For example, the radius of a molecule must increase 8–10-fold to decrease *D* by one half. The reduction of *D* for the mutant proteins by one third to one half is consistent with the biochemical data indicating that the mutants oligomerize through intermolecular disulfide bridges and associate with calnexin and potentially with other chaperones. In addition, the retention of mobile misfolded complexes is similar to the results observed by Nehls *et al.* (49) for misfolded VSVG and by Haggie *et al.* (50) for misfolded CFTR. Retention is likely to be due to exclusion of the large protein/chaperone complexes from ER exit sites by an uncharacterized mechanism.

DISCUSSION

Chaperones in the ER perform an essential role in ensuring quality control of the proper folding of polytopic proteins (38, 39). Proteins that fail to correctly fold and remain associated

with chaperones for prolonged periods generally cannot exit from the ER. Both this study and work by others clearly demonstrate that wt Gas3/PMP22 associates transiently with the chaperone CNX during protein folding in the ER (18, 42). In this study, we have provided new insights into the molecular nature of the interaction of CNX with both wt and mutant variants of Gas3/PMP22.

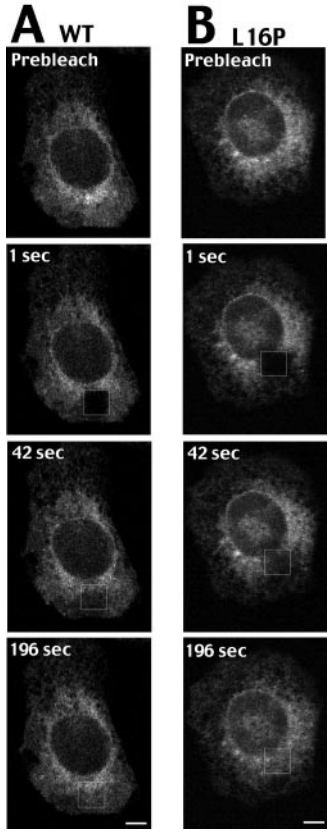

FIG. 7. **Diffusional mobility of wt and the L16P mutant within ER membranes.** Qualitative FRAP analysis of wt (*A*) expressed in cells grown in the presence of brefeldin A or of L16P (*B*). Cells were photobleached in a small ROI (*outlined box*) and monitored for recovery of fluorescence into the ROI. The two proteins appear mobile and recover fully. *Bars*, 8 μm.

The critical role of *N*-linked glycans in the regulation of ER quality control of glycoproteins is well established (20, 52). Less is known about whether and how the lectin chaperone quality control machinery associates with non-glycosylated proteins. Several studies have provided evidence that the lectin chaperones, CNX and CRT, can associate with unfolded molecules through direct protein-protein interactions in the absence of the $Glc_1Man_9GlcNAc_2$ oligosaccharide (36–39, 53–55).

In the case of wt, interaction with CNX depends directly on the presence of the sugar moiety. Although the N41Q glycosylation mutant folds and functions normally (13), it does not associate with CNX. In contrast, the misfolded mutant L16P, regardless of *N*-glycosylation status, stably associates with CNX. Thus, CNX association displays different requirements for the oligosaccharide, depending on the presence of misfolding mutations. The interaction between CNX and the L16P/N41Q mutant was not a consequence of nonspecific aggregation or of the GFP tag. The L16P/N41Q mutant was nearly completely soluble when extracted in the presence of CHAPS or Triton X-100 detergents in the co-IP studies. Furthermore, the glycan-independent interaction of L16P mutant with CNX was unaffected by the absence of interchain oligomer formation by disulfide bonds during DTT treatment. Finally, this interaction also was observed in the presence of FLAG-tagged mutants.

What domains of non-glycosylated proteins does CNX recognize as misfolded? We have demonstrated that TM1 of either wt or L16P was able to interact with CNX and was retained in the ER. Interestingly, other tetraspan proteins can interact with CNX through their transmembrane domains. A mutant of CD82 lacking its first TM domain or expression of the first TM domain alone results in CNX association and ER retention (38). Similarly, an isolated TM domain of proteolipid protein is retained in the ER and interacts with CNX (39). Therefore, our data provide support for an emerging model in which CNX can recognize improperly folded transmembrane domains. Single TM domains of polytopic proteins may be recognized by CNX as misfolded due to the presence of polar residues that normally assist the packing of the TM domains together (56). Interestingly, polar residues are common in the TM domains of poly-

TABLE I

D_{eff} and M_f values for ER-localized Gas3/PMP22-GFP fusion proteins

Means ± S.D. of values for D_{eff} and M_f for FRAP experiments of cells expressing the indicated fusion proteins. *n* = number of experiments. BFA, brefeldin A.

Chimera	Treatment	D_{eff}	M_f	*n*
		$\mu m^2/s$		
Gas3/PMP22-GFP	BFA	0.54 ± 0.14	94 ± 6.8	9
Gas3/PMP22-N41Q-GFP	BFA	0.64 ± 0.19	93 ± 6.2	9
Gas3/PMP22-L16P-GFP	None	0.29 ± 0.07[a]	87 ± 7.2	10
Gas3/PMP22-L16P/N41Q-GFP	None	0.28 ± 0.12[a]	89 ± 5.7	10
Sec61γ-GFP	None	0.51 ± 0.15	92 ± 2.0	6

[a] $p \leq 0.01$ relative to wt.

TABLE II

D_{eff} and M_f values for ER-localized Gas3/PMP22 mutants

Means ± S.D. of values for D_{eff} and M_f for FRAP experiments of cells expressing the indicated fusion proteins. *n* = number of experiments. BFA, brefeldin A.

Chimera	Treatment	D_{eff}	M_f	*n*
		$\mu m^2/s$		
Gas3/PMP22-GFP	BFA	0.53 ± 0.07	96 ± 5.1	4
Gas3/PMP22-C109R-GFP	None	0.39 ± 0.09[a]	94 ± 6.2	9
Gas3/PMP22-G150D-GFP	None	0.31 ± 0.08[b]	91 ± 8.0	8
Gas3/PMP22-S72L-GFP	None	0.37 ± 0.10[a]	94 ± 5.1	8

[a] $p \leq 0.01$ relative to wt.
[b] $p \leq 0.05$ relative to wt.

topic proteins but rare in the TM domains of single-spanning membrane proteins (39, 56, 57). The TM1 of Gas3/PMP22 contains polar and charged residues, which provides support for this hypothesis.

In the absence of lectin binding, how might CNX interact with misfolded transmembrane domains? When unfolded glycoproteins interact with both the lectin site and a polypeptide-binding site of CNX, as suggested in the "dual binding" model (37), the polypeptide-binding site serves to suppress aggregation of the unfolded substrate (37, 55, 58). It is unclear which segment of CNX contains the polypeptide-binding site, but a role of the TM domain of CNX in monitoring the assembly of transmembrane domains is suggested by recent studies (38, 39). Interestingly, we observed that the lectin chaperone CRT, which is similar to CNX but lacks the TM domain, is recruited to the L16P mutant-induced aggresomes but not to *N*-glycosylation-defective mutant L16P/N41Q-induced aggresomes.[2] Our data suggest a potential role for the TM domain of CNX in recognizing and binding to the misfolded TM domains of polytopic proteins. Alternatively, the interaction of CNX with the misfolded L16P mutant lacking the sugar moiety may be mediated by the CNX binding partner, ERp57 (21). However, this possibility is unlikely because growing cells in the presence of 2.5 mM DTT for 30 min before extraction for IP does not inhibit the binding of CNX to the L16P/N41Q mutant.

Finally, we investigated how misfolded Gas3/PMP22 is retained in the ER. FRAP analysis revealed that whereas both wt and mutant forms of Gas3/PMP22 are mobile, the mutant forms exhibit significantly lower D_{eff} values than the wt. The lower D_{eff} values independently confirm incorporation of the misfolded mutants into high molecular weight complexes and/or the enhanced association with ER chaperones in living cells. The diffusional mobility of misfolded and folded proteins in the ER has been investigated previously by using a temperature-sensitive variant of VSVG protein (49) and the ΔF508 mutant of CFTR (50). As with Gas3/PMP22, the folded and misfolded forms of VSVG and CFTR exhibited high M_f values. In contrast to Gas3/PMP22, the D_{eff} values for folded and misfolded forms of VSVG and CFTR were indistinguishable, even though misfolded VSVG and ΔF508CFTR also interact with CNX (49, 50). At least two factors could account for the differences in D_{eff} values. First, the misfolding mutations of VSVG and ΔF508CFTR are lumenal amino acids, whereas the Gas3/PMP22 mutations involve amino acids within predicted transmembrane domains. It is possible that the chaperones could interact with the resulting misfolded domains with different dynamics. For example, association of CNX with VSVG or CFTR may occur with bind and release kinetics, whereas CNX may stably bind mutant Gas3/PMP22. Second, L16P clearly forms larger interchain aggregates, whereas the size of misfolded VSVG complexes is unknown. Despite the differences in D_{eff} values, the key finding is that misfolded ER-retained mutants of VSVG, CFTR, and Gas3/PMP22 are not immobilized. Thus, ER retention of misfolded membrane proteins appears to be mediated by a general mechanism of exclusion from ER exit sites.

In conclusion, our studies have provided new insights into the mechanism of ER retention of Gas3/PMP22. We have described a new mode of CNX-mediated retention for Gas3/PMP22 and suggest that Gas3/PMP22 provides an excellent model to study the relationships among CNX, protein misfolding, and ER retention. Dissecting these relationships will be critical for a number of diseases exhibiting defects in protein folding and ER exit.

[2] A. Fontanini, R. Chies, E. L. Snapp, M. Ferrarini, G. M. Fabrizi, and C. Brancolini, unpublished data.

Acknowledgments—We thank R. Halaban (New Haven, CT) for pEGFP-TYR/T373K, R. Sitia (Milan, Italy) for anti-ERp44 antibody, and M. Stebel (Trieste, Italy) for helping prepare antibodies. We also thank P. Edomi (Trieste, Italy) for some help in generating Gas3/PMP22 plasmids, E. D. Siggia (New York, NY) for the diffusion simulation program, and E. di Centa (Udine, Italy) for sequencing service. We are grateful to F. Demarchi (Trieste, Italy) for critical reading of the manuscript.

REFERENCES

1. Spreyer, P., Kuhn, G., Hanemann, C. O., Gillen, C., Schaal, H., Kuhn, R., Lemke, G., and Muller, H. W. (1991) *EMBO J.* **10,** 3661–3668
2. Welcher, A. A., Suter, U., De Leon, M., Snipes, G. J., and Shooter, E. M. (1991) *Proc. Natl. Acad. Sci. U. S. A.* **88,** 7195–7199
3. Snipes, G. J., Suter, U., Welcher, A. A., and Shooter, E. M. (1992) *J. Cell Biol.* **117,** 225–238
4. Patel, P. I., and Lupski, J. R. (1994) *Trends Genet.* **10,** 128–133
5. Suter, U., and Snipes, G. J. (1995) *Annu. Rev. Neurosci.* **18,** 45–75
6. Naef, R., and Suter, U. (1998) *Res. Tech.* **41,** 359–371
7. De Jonghe, P., Timmerman, V., Nelis, E., Martin, J. J., and Van Broeckhoven, C. (1997) *J. Peripher. Nerv. Syst.* **2,** 370–387
8. Meuleman, J., Pou-Serradell, A., Lofgren, A., Ceuterick, C., Martin, J. J., Timmerman, V., Van Broeckhoven, C., and De Jonghe, P. (2001) *Neuromuscul. Disord.* **11,** 400–403
9. Nelis, E., Haites, N., and Van Broeckhoven, C. (1999) *Hum. Mutat.* **13,** 11–28
10. D'Urso, D., Prior, R., Greiner-Petter, R., Gabreels-Festen, A. A., and Muller, H. W. (1998) *J. Neurosci.* **18,** 731–740
11. Naef, R., and Suter, U. (1999) *Neurobiol. Dis.* **6,** 1–14
12. Tobler, A. R., Notterpek, L., Naef, R., Taylor, V., Suter, U., and Shooter, E. M. (1999) *J. Neurosci.* **19,** 2027–2036
13. Brancolini, C., Edomi, P., Marzinotto, S., and Schneider, C. (2000) *Mol. Biol. Cell* **11,** 2901–2914
14. Muller, H. W. (2000) *Glia* **29,** 182–185
15. Sanders, C. R., Ismail-Beigi, F., and McEnery, M. W. (2001) *Biochemistry* **40,** 9453–9459
16. Isaacs, A. M., Jeans, A., Oliver, P. L., Vizor, L., Brown, S. D., Hunter, A. J., and Davies, K. E. (2002) *Mol. Cell. Neurosci.* **21,** 114–125
17. Tobler, A. R., Liu, N., Mueller, L., and Shooter, E. M. (2002) *Proc. Natl. Acad. Sci. U. S. A.* **99,** 483–488
18. Dickson, K. M., Bergeron, J. J., Shames, I., Colby, J., Nguyen, D. T., Chevet, E., Thomas, D. Y., and Snipes, G. J. (2002) *Proc. Natl. Acad. Sci. U. S. A.* **99,** 9852–9857
19. Cabral, C. M., Liu, Y., and Sifers, R. N. (2001) *Trends Biochem. Sci.* **26,** 619–624
20. Ellgaard, L., and Helenius, A. (2001) *Curr. Opin. Cell Biol.* **13,** 431–437
21. Ellgaard, L., and Helenius, A. (2003) *Nat. Rev. Mol. Cell. Biol.* **4,** 181–191
22. Trombetta, E. S., and Parodi, A. J. (2003) *Annu. Rev. Cell Dev. Biol.* **19,** 649–676
23. Hammond, C., Braakman, I., and Helenius, A. (1994) *Proc. Natl. Acad. Sci. U. S. A.* **91,** 913–917
24. Parodi, A. J. (2000) *Annu. Rev. Biochem.* **69,** 69–93
25. Trombetta, E. S., and Helenius, A. (2000) *J. Cell Biol.* **148,** 1123–1129
26. Chies, R., Nobbio, L., Edomi, P., Schenone, A., Schneider, C., and Brancolini, C. (2003) *J. Cell Sci.* **116,** 987–999
27. Snapp, E. L., Hegde, R. S., Francolini, M., Lombardo, F., Colombo, S., Pedrazzini, E., Borgese, N., and Lippincott-Schwartz, J. (2003) *J. Cell Biol.* **163,** 257–269
28. Brown, D. A., and Rose, J. K. (1992) *Cell* **68,** 533–544
29. Paroni, G., Mizzau, M., Henderson, C., Del Sal, G., Schneider, C., and Brancolini, C. (2004) *Mol. Biol. Cell* **15,** 2804–2818
30. Siggia, E. D., Lippincott-Schwartz, J., and Bekiranov, S. (2000) *Biophys. J.* **79,** 1761–1770
31. Snapp, E. L., Altan, N., and Lippincott-Schwartz, J. (2003) in *Current Protocols in Cell Biology* (Bonifacino, J., Dasso, M., Harford, J.B., Lippincott-Schwartz, J., and Yamada, K. M., eds) pp. 21.1.1–21.1.23, John Wiley and Sons, Inc., New York
32. Anelli, T., Alessio, M., Mezghrani, A., Simmen, T., Talamo, F., Bachi, A., and Sitia, R. (2002) *EMBO J.* **21,** 835–844
33. Fabbretti, E., Edomi, P., Brancolini, C., and Schneider, C. (1995) *Genes Dev.* **9,** 1846–1856
34. Helenius, A., and Aebi, M. (2001) *Science* **291,** 2364–2369
35. Hebert, D. N., Foellmer, B., and Helenius, A. (1995) *Cell* **81,** 425–433
36. Cannon, K. S., Hebert, D. N., and Helenius, A. (1996) *J. Biol. Chem.* **271,** 14280–14284
37. Ihara, Y., Cohen-Doyle, M. F., Saito, Y., and Williams, D. B. (1999) *Mol. Cell* **4,** 331–341
38. Cannon, K. S., and Cresswell, P. (2001) *EMBO J.* **20,** 2443–2453
39. Swanton, E., High, S., and Woodman, P. (2003) *EMBO J.* **22,** 2948–2958
40. Notterpek, L., Ryan, M. C., Tobler, A. R., and Shooter, E. M. (1999) *Neurobiol. Dis.* **6,** 450–460
41. Ryan, M. C., Shooter, E. M., and Notterpek, L. (2002) *Neurobiol. Dis.* **10,** 109–118
42. Shames, I., Fraser, A., Colby, J., Orfali, W., and Snipes, G. J. (2003) *J. Neuropathol. Exp. Neurol.* **62,** 751–764
43. Erne, B., Sansano, S., Frank, M., and Schaeren-Wiemers, N. (2002) *J. Neurochem.* **82,** 550–562
44. Hasse, B., Bosse, F., and Muller, H. W. (2002) *J. Neurosci. Res.* **69,** 227–232
45. Simons, K., and Ehehalt, R. (2002) *J. Clin. Investig.* **110,** 597–603
46. Marquardt, T., and Helenius, A. (1992) *J. Cell Biol.* **117,** 505–513
47. Dangoria, N. S., DeLay, M. L., Kingsbury, D. J., Mear, J. P., Uchanska-Ziegler, B., Ziegler, A., and Colbert, R. A. (2002) *J. Biol. Chem.* **277,** 23459–23468
48. Halaban, R., Svedine, S., Cheng, E., Smicun, Y., Aron, R., and Hebert, D. N.

(2000) *Proc. Natl. Acad. Sci. U. S. A.* **97,** 5889–5894
49. Nehls, S., Snapp, E. L., Cole, N. B., Zaal, K. J., Kenworthy, A. K., Roberts, T. H., Ellenberg, J., Presley, J. F., Siggia, E., and Lippincott-Schwartz, J. (2000) *Nat. Cell Biol.* **2,** 288–295
50. Haggie, P. M., Stanton, B. A., and Verkman, A. S. (2002) *J. Biol. Chem.* **277,** 16419–16425
51. Hughes, B. D., Pailthorpe, B. A., White, J. R., and Sawyer, W. H. (1982) *Biophys. J.* **37,** 673–676
52. Trombetta, E. S. *Glycobiology* (2003) **13,** 77R–91R
53. Saito, Y., Ihara, Y., Leach, M. R., Cohen-Doyle, M. F., and Williams, D. B. (1999) *EMBO J.* **18,** 6718–6729
54. Danilczyk, U. G., and Williams, D. B. (2001) *J. Biol. Chem.* **276,** 25532–25540
55. Stronge, V. S., Saito, Y., Ihara, Y., and Williams, D. B. (2001) *J. Biol. Chem.* **276,** 39779–39787
56. Reggiori, F., and Pelham, H. R. (2002) *Nat. Cell Biol.* **4,** 117–123
57. Sato, K., Sato, M., and Nakano, A. (2001) *J. Cell Biol.* **152,** 935–944
58. Leach, M. R., Cohen-Doyle, M. F., Thomas, D. Y., and Williams, D. B. (2002) *J. Biol. Chem.* **277,** 29686–29697
59. Taylor, V., Zgraggen, C., Naef, R., and Suter, U. (2000) *J. Neurosci. Res.* **62,** 15–27